Journal of Nuclear Materials 394 (2009) 144–150

Contents lists available at ScienceDirect

Journal of Nuclear Materials

journal homepage: www.elsevier.com/locate/jnucmat

Performance of a diffusion barrier under a fuel–clad chemical interaction (FCCI)

Jun Hwan Kim [a,*], Ho Jin Ryu [a], Jong Hyuk Baek [a], Seok Jin Oh [a], Byoung Oon Lee [a], Chan Bock Lee [a], Young Soo Yoon [b,**]

[a] Recycled Fuel Development Division, Korea Atomic Energy Research Institute, P.O. Box 105, Yuseong, Daejeon 305-600, Republic of Korea
[b] Department of Materials Science and Engineering, Yonsei University, 134 Sinchon Dong, Seoul 120-749, Republic of Korea

ARTICLE INFO

Article history:
Received 3 November 2008
Accepted 29 August 2009

Keywords:
Fuel–clad chemical interaction (FCCI)
Vapor deposition
Metallic fuel
Diffusion
Barrier

ABSTRACT

Studies were carried out to assess the performance of a vapor deposition as a diffusion barrier under a fuel–clad chemical interaction (FCCI). Single or multiple layers of zirconium, chromium and titanium were coated onto a HT9 clad surface and diffusion couple tests at 800 °C for 25 h were carried out for a U–10 wt%Zr metallic fuel. While a massive reaction occurred at the fuel–clad interface for the specimen without any surface treatment, the vapor-deposited specimens showed an excellent resistance against a FCCI regardless of the coating materials. Specimen coated with zirconium remained intact. However, the coating consists of the multiple layers with titanium, chromium and zirconium dissolved and formed as a precipitate at a fuel interface after the diffusion couple test. Although it dissolved and precipitated as small-sized particles during the diffusion test, secondary zirconium-rich phase preferentially agglomerated around the particles, which acted as a barrier against FCCI.

1. Introduction

Metallic fuel has been considered as one of the most probable candidates for the fuel system in the sodium-cooled fast reactor (SFR) in that it has high thermal conductivity, proliferation resistance, ease of fabrication and good compatibility for sodium [1]. The addition of an alloying element such as chromium, molybdenum, zirconium and titanium has been applied in order to increase the solidus temperature of the uranium–plutonium alloy. Among these, uranium–plutonium alloys with the addition of 10–20 wt% zirconium have been considered in the design of the metallic fuel for a SFR. However, actinide elements in a metallic fuel like uranium and plutonium react with austenitic or ferritic–martensitic stainless steel at a temperature above 650 °C to form eutectic compounds [2]. Such a eutectic reaction reduces the cladding thickness so that the mechanical integrity of the cladding gradually decreases as the fuel burnup proceeds. To mitigate such a circumstance, a barrier layer, which prevents both the fuel and clad elements from diffusing into each other, has been proposed. Metallic foil made of pure metal has been suggested as a barrier and its feasibility test has been carried out [3,4]. To provide a wide selection of the barrier, a surface treatment of a material has been proposed to induce the formation of a protective layer that improves the surface property [5,6]. Vapor deposition is one of the surface treatment processes where the reactant deposits over the surface of a target material either physically or chemically under controlled conditions [7]. It has been widely used for enhancing surface properties such as a corrosion, wear, electrical conductivity and diffusion resistance [8–10]. Since it is expected to apply to the inner surface of the cladding much easier than the metallic foil alone, it can be effectively used for suppressing a fuel–clad chemical interaction (FCCI) provided that the optimum conditions are found. The objectives in this study are to propose the possibility of a vapor deposition as a type of the barrier and to verify its performance under a fuel–clad interaction situation.

2. Experimental

2.1. Specimen preparation

Both an uranium–zirconium alloy and a HT9 were used as a metallic fuel and a clad material in this study. Table 1 showed the chemical composition of the test material. The metallic fuel rod was fabricated from uranium and zirconium lumps by induction melting. Fuel rod was furnace-cooled after melting in zirconia crucibles. HT9 has been fabricated by vacuum induction melting. Specimens were prepared as a 6.6 mm disk for the fuel and an 8 mm disk for the clad, respectively, prior to the test.

2.2. Vapor deposition process

After specimen preparation, vapor deposition process was carried out. Chromium and zirconium were selected as the main component of the layer material because they have been found to be

* Corresponding author. Tel.: +82 42 868 8623; fax: +82 42 868 8709.
** Corresponding author. Tel.: +82 2 2123 2847; fax: +82 2 365 5882.
E-mail addresses: junhkim@kaeri.re.kr (J.H. Kim), yoonys@yonsei.ac.kr (Y.S. Yoon).

0022-3115/$ - see front matter © 2009 Elsevier B.V. All rights reserved.
doi:10.1016/j.jnucmat.2009.08.018

Table 1
Chemical composition of the test material (measured value).

HT9	C	Si	Mn	Cr	Ni	Mo	W	V	Nb	N	Fe
Wt%	0.19	0.14	0.49	12.05	0.48	1.00	0.49	0.30	0.02	0.01	Bal.
U–10Zr[a]		Zr		C		H		O			U
Wt%		10.1		0.12		0.09		0.54			Bal.

[a] 119 ppm of Fe and 12 ppm of Ni were incorporated as an impurity.

superior against FCCI from the previous paper [3]. Commercial chromium alloy, which contains a small amount of nickel, and zirconium metal were used as a source in the vapor deposition. The vapor deposition method adopted in this study was a direct-current magnetron sputtering whose deposition condition is shown in Table 2. The barrier layer in this study were constructed as follows; One was a zirconium layer coated onto a clad surface with a thickness of 6 μm (noted as VD #1). Another was a composite of a chromium alloy and a zirconium layer alternately coated 5 times onto a clad surface with a thickness of 6 μm (noted as VD #2). The third has the same layer structure as VD #2 except for a 150 nm-thick titanium layer coated between the first chromium alloy layer and the clad material. Titanium was selected because it is expected to act as a buffer layer. The structure of each layer was described in Table 3. After deposition, the structure of the barrier layer was examined through scanning electron microscopy (SEM) and the Auger electron spectroscopy (AES), where it was revealed that the thickness as well as the composition of the layer was developed well over the clad surface, like in Fig. 1.

2.3. Diffusion couple test

To assess the performance of the barrier, diffusion couple tests between the metallic fuel and the clad material were carried out. Metallic fuel disk and the vapor-deposited clad disk were contacted with each other. Then the coupled specimen was inserted into the screw-type jig made of 316-type stainless steel and then it was clamped. The coupled specimen was wrapped with a tantalum foil to avoid any unnecessary reaction between the specimen and the jig. After clamping, they were placed in the vacuum furnace then the diffusion couple tests were performed. Tests were at a temperature of 800 °C for 25 h, which was higher than the normal operation temperature of a SFR, 650 °C. As the main objective in this study is to test the performance of the barrier layer under the FCCI condition, it was intended to raise the test temperature as the normal case in order to evaluate the endurance of the barrier in an efficient way by relatively short time. Also, since metallic fuel in this study does not contain plutonium, it was necessary to raise the temperature in order to compensate for the effect of the plutonium, which decreases the onset temperature to induce FCCI [3]. After testing, the specimens were pulled out of the furnace and quenched in water to prevent any microstructural changes or an oxidation during slow cooling of the specimen in an air environment. Fig. 2 shows the schematic illustration of the diffusion test. After the test, the specimens were sectioned, mounted and ground up to 2000 grit, followed by a SEM/EDX analysis. Intensities of each element were obtained and they were converted into an atomic percent. (Hereafter, % denotes at.% unless otherwise mentioned.) Table 4 summarized the element contents of the specimen after the diffusion couple test.

3. Results and discussion

3.1. Diffusion couple test result

Fig. 3 shows the microstructure of the specimen without the diffusion barrier after the diffusion couple test at 800 °C for 25 h, where it showed that a massive reaction occurred for the fuel–clad coupled specimen. Uranium and zirconium diffused toward the clad material to encroach on the cladding material to form a reaction layer, whose thickness was approximately 250 μm. (Note the layer between the interface and the clad in Fig. 3.) Also, iron and chromium diffused toward the fuel to form a complex phase in the metallic fuel. In the case of the vapor-deposited specimen, no visible reaction could be seen at the fuel–clad interface. In the VD #1 specimen, as in Fig. 5, the metallic fuel and the clad disk bonded with each other after disassembly of the jig after the test. In the VD #2 and #3 specimens, the metallic fuel and the clad disk were found to be detached from each other, as in Figs. 6 and 7. Since no bonding caused by the significant eutectic reaction occurred in the surface-treated specimen, it is concluded that vapor deposition can be applied as one of the probable methods for preventing a FCCI. To evaluate the performance of the each diffusion barrier in terms of a fuel element penetration, the uranium and zirconium contents were measured for the cladding, just below a 10 μm depth from the fuel–clad interface. Fig. 8 shows the result of the element content at that position. In the specimen without diffusion barrier, uranium and zirconium were diffused into the cladding so that their contents 10 μm beneath the interface were respectively 25.83% and 5.22%. In the vapor-deposited specimens, the uranium content was significantly reduced to a value of 0.55% in the VD #1 specimen, 0.1% in the VD #2 specimen, and 0.17% in the VD #3

Table 3
Vapor deposition conditions in this study.

Sample name	Layer structure	Total thickness
Ref.	Clad | w/o barrier	
VD #1	Clad | Zr layer	~6 μm
VD #2	Clad | (Cr_Ni alloy–Zr) × 5 layer	~6 μm
VD #3	Clad | Ti–(Cr_Ni alloy–Zr) × 5 layer	~6 μm (Ti layer: ~150 nm)

Table 2
Deposition condition of the barrier layer in this study.

	Sputter power	Working pressure (Pa)	Gas composition (flow rate)	Deposition time (min)	Temperature
Ti layer	200 W (0.44–0.5 A)	6.7×10^{-4}	Ar (40 cm^3/min)	10	Room temperature
Cr_Ni layer	200 W (0.44–0.5 A)	6.7×10^{-4}	Ar (40 cm^3/min)	10	Room temperature
Zr layer	200 W (0.44–0.5 A)	6.7×10^{-4}	Ar (40 cm^3/min)	45	Room temperature

specimen. Zirconium content was also suppressed in the case of the surface-treated specimen. In the VD #2 specimen, zirconium was not found at the cladding. Although the zirconium content in the VD #3 specimen was not negligible, its value was still below the reference condition, showing that a vapor deposition process has an effect of suppressing an inter-diffusion between the metallic fuel and the cladding.

3.2. Microstructural analysis of specimens

Fig. 5 shows a magnified image of the specimen without a vapor deposition after the diffusion couple test at 800 °C for 25 h. To identify the phase at each region, a composition analysis at a selective point by EDX, and by collating it with a ternary phase diagram proposed by Nakamura [11], was carried out. For simplicity, the iron and the chromium were regarded as a single element. Iron and chromium diffuse toward the fuel side to form the intermediate compound as $U(Fe,Cr)_2$ (point 1 in Fig. 4(a)) and $Zr(Fe,Cr)_2$ (point 2 in Fig. 4(a)) in the liquid phase (point 3 in Fig. 4(a)). These phases reacted together and converted into the another intermediate phase like $U(Fe,Cr)_2 + Zr(Fe,Cr)_2 + Zr_6(Fe,Cr)_{23}$ (point 1 in Fig. 4(b)) in the liquid phase (point 2 in Fig. 4(b)). In the region below the fuel–clad interface, the iron concentration was relatively high so that α-Fe + $U(Fe,Cr)_2$ + $Zr_6(Fe,Cr)_{23}$ consist the reaction layer (refer to the point e in Fig. 4(c)).

Fig. 5 shows the microstructural observation of the interface between the U–10Zr and the VD #1-treated clad. In a comparison with the specimen without vapor deposition process, no visible phase formation caused by inter-diffusion was found across the barrier layer. In the EDX analysis, however, small amount of diffusion was indicated between the metallic fuel and the clad material. 5.48% of chromium and 8.21% of iron were found in the metallic fuel at the vicinity of an interface (point a in Fig. 6). At point c in Fig. 7, uranium was not found in the clad material. Although a small amount of zirconium at 1.21% was found in the clad material, it is not known whether the detected zirconium originated from the dissolution of the initially deposited layer or the diffusion of the metallic fuel.

Fig. 6 shows the microstructural observation of the cross-sectional image of the fuel and the VD #2 specimen. Similar to the case of VD #1, no apparent phase formation was found at either the fuel or the cladding side. However, the barrier layer disappeared either at

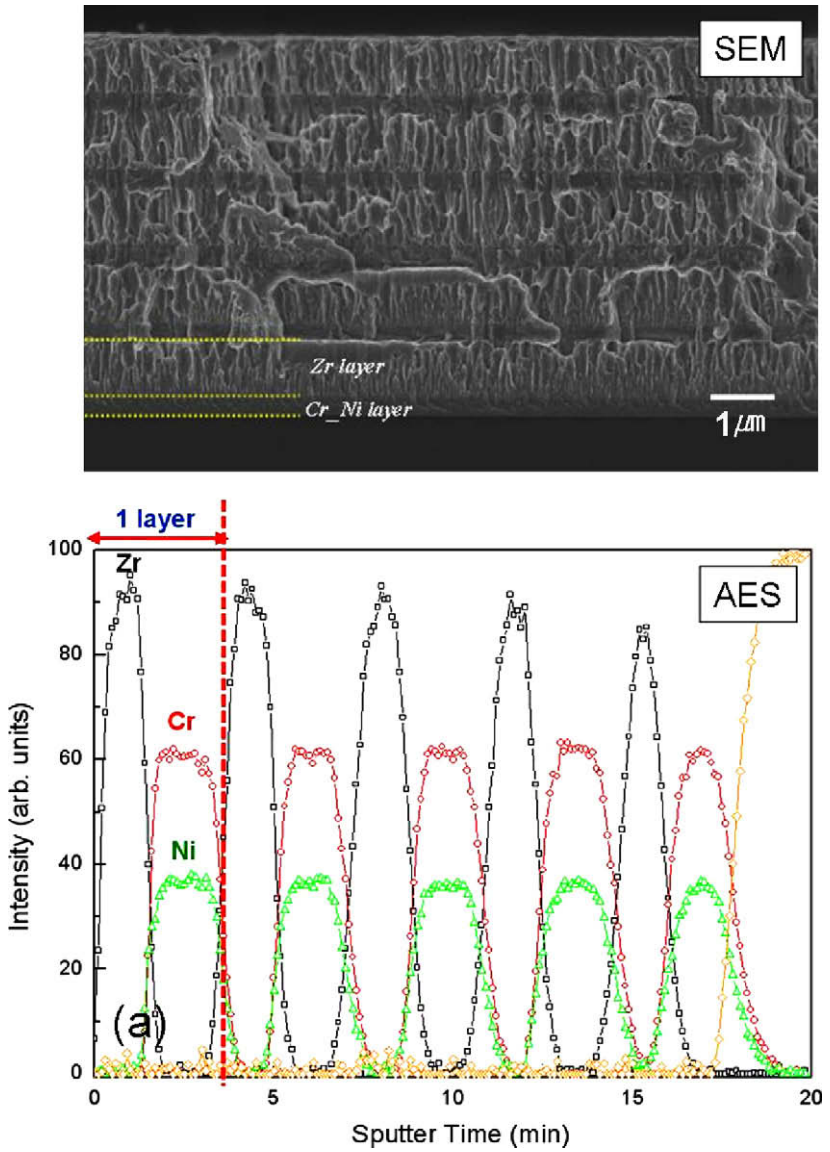

Fig. 1. Characterization of the vapor-deposited layer on the clad material. (a) VD #2, (b) VD #3.

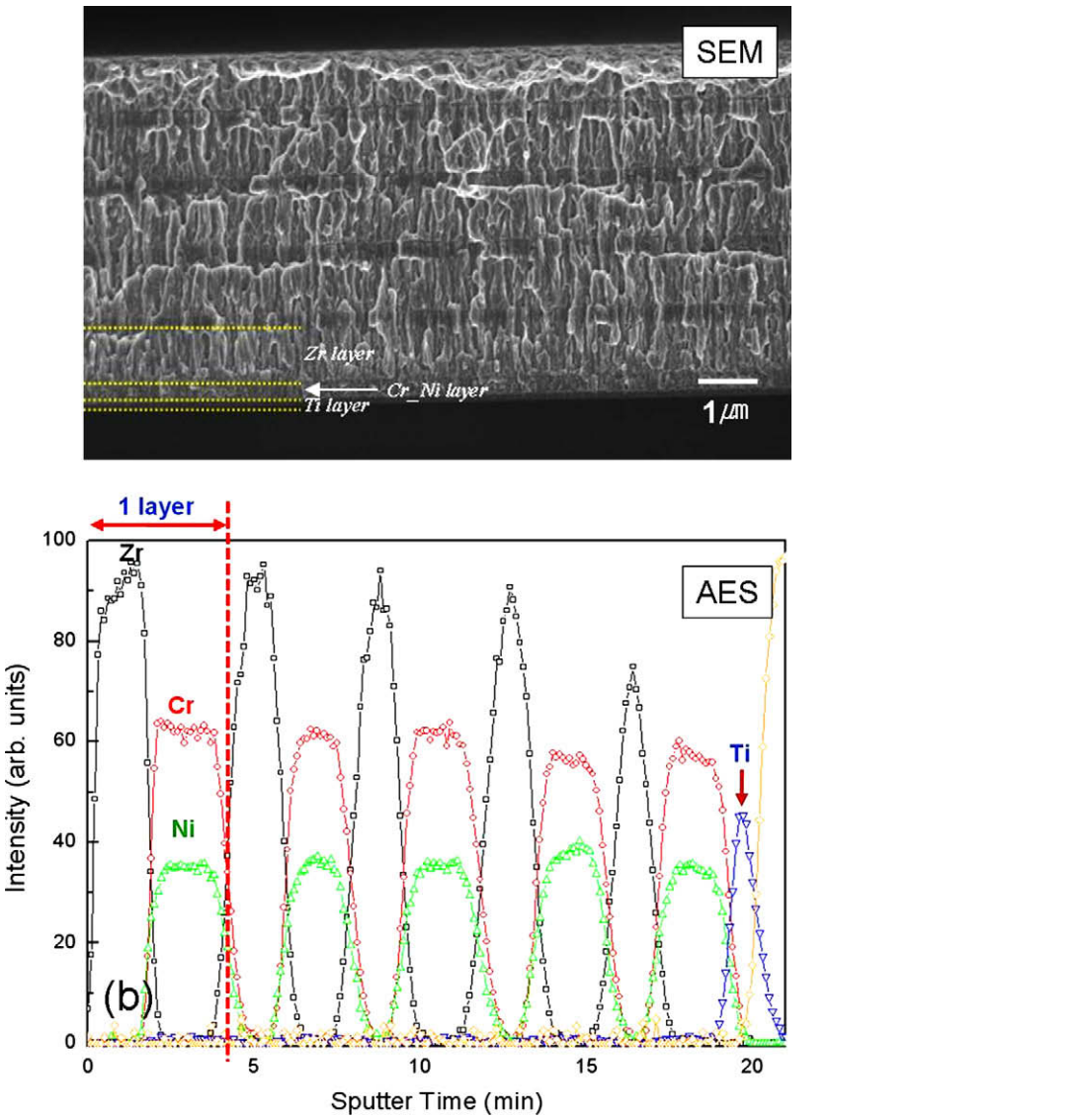

Fig. 1 (*continued*)

the fuel or the clad and small particles remained in the fuel side. EDX analysis of the particles revealed that they were composed of uranium which contained 23 at.% zirconium mixed with a small amount of chromium, iron and nickel. Thus it is assumed that chromium, iron and nickel inside the barrier layer dissolved and formed as particles. Besides the small-sized particles, a zirconium-enriched phase appeared at the interface of the fuel side. (Refer to the point e in Fig. 6(a).) Since zirconium is known to give an increased resistance to a FCCI by increasing the solidus temperature of a metallic fuel [12], such a formed zirconium phase may act as a barrier against a diffusion of the uranium. Similar result has been proposed in a previous paper [13] that such a zirconium layer may have originated from a decomposition of the δ-phase of a metallic fuel and a preferential redistribution of a zirconium element at a discontinuous site such as the surface of the fuel. Suppose that the formation of the zirconium phase is initiated by an unstable site such as an interface, the particle generated by the dissolution of the vapor-deposition layer can accelerate the precipitation of the protective zirconium phase. It is reported that chromium inside a particle has an influence on the formation of the zirconium phase [12]. If the clad material contained a higher chromium level, it favors the formation of a highly enriched zirconium phase.

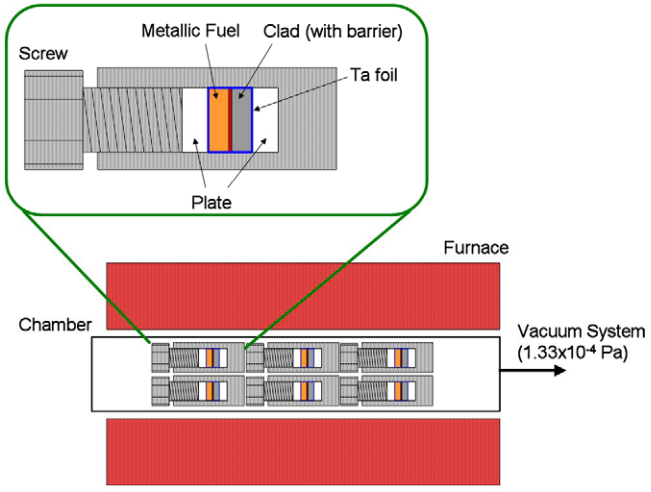

Fig. 2. Schematic illustration of the diffusion couple test.

Table 4
Element content of the specimen after diffusion test at 800 °C for 25 h (selective points).

Specimen	Region	Location	Element (at.%)
Ref. (w/o barrier)	Fig. 4(a)	a	7.88Zr–24.32U–10.62Cr–57.18Fe
		b	19.25Zr–14.08U–16.49Cr–50.19Fe
		c	1.54Zr–76.77U–1.49Cr–20.20Fe
		d	16.05Zr–17.62U–14.00Cr–52.32Fe
	Fig. 4(b)	a	7.17Zr–24.07U–10.93Cr–57.82Fe
		b	97.20Zr–0.85U–0.56Cr–1.39Fe
		c	8.18Zr–23.21U–10.36Cr–58.25Fe
		d	5.22Zr–25.83U–11.17Cr–57.78Fe
	Fig. 4(c)	a	3.27Zr–28.08U–9.37Cr–59.28Fe
		b	3.85Zr–27.02U–10.25Cr–58.88Fe
		c	1.56Zr–28.59U–7.98Cr–61.87Fe
		d	0.47U–15.25Cr–84.28Fe
		e	0.12U–13.07Cr–86.81Fe
VD #1	Fig. 5	a	29.86Zr–56.63U–5.48Cr–8.21Fe
		b	89.71Zr–2.57U–2.64Cr–5.09Fe
		c	1.21Zr–0.55U–13.62Cr–84.62Fe
VD #2	Fig. 6(a)	a	18.68Zr–77.10Cr–1.46Cr–2.76Fe
		b	21.89Zr–69.39U–2.25Cr–2.80Fe–3.67Ni
		c	20.08Zr–71.25U–1.93Cr–3.10Fe–3.64Ni
		d	22.56Zr–71.12U–0.82Cr–2.35Fe–3.15Ni
		e	73.32Zr–22.04U–0.69Cr–1.26Fe–2.69Ni
	Fig. 6(b)	a	50.42Zr–2.72U–19.09Cr–26.96Fe–0.81Ni
		b	13.60Zr–0.47U–29.87Cr–55.51Fe–0.55Ni
		c	6.13Zr–0.20U–27.50Cr–65.94Fe–0.23Ni
		d	0.10U–13.33Cr–86.30Fe–0.27Ni
VD #3	Fig. 7(a)	a	9.83Zr–81.47U–1.45Ti–1.68Cr–3.03Fe–2.54Ni
		b	4.95Zr–88.46U–0.43Ti–1.45Cr–2.42Fe–2.28Ni
		c	90.80Zr–5.29U–0.89Ti–0.77Cr–1.28Fe–0.98Ni
		d	95.62Zr–1.39U–0.91Ti–0.51Cr–0.82Fe–0.76Ni
	Fig. 7(b)	a	41.41Zr–15.13U–4.44Ti–14.70Cr–23.19Fe–1.13Ni
		b	1.57Zr–0.31U–1.09Ti–11.86Cr–85.03Fe–0.13Ni
		c	0.30Zr–0.21U–0.11Ti–12.53Cr–86.32Fe–0.53Ni

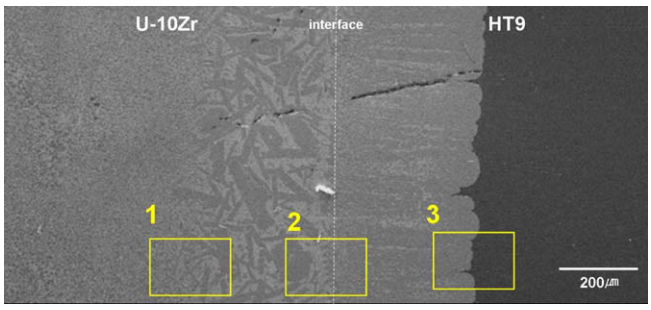

Fig. 3. Microstructure of the specimen without diffusion barrier after diffusion couple test at 800 °C for 25 h.

The effect of vapor deposition on the precipitation of a zirconium-rich phase is more apparent when titanium is added to the barrier layer. Fig. 7 shows the microstructural observation of the VD #3-treated specimen after a diffusion couple test. As in the previous results, it did not show any bonding caused by the eutectic reaction, nor any inter-diffusion at either the fuel or the clad side.

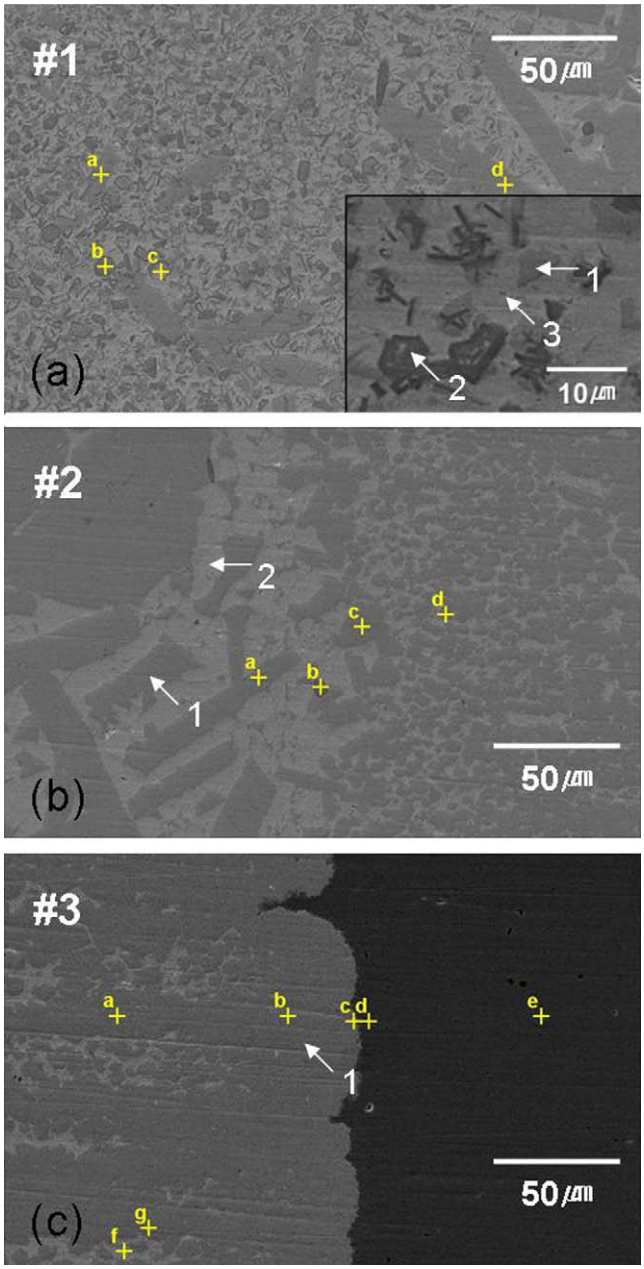

Fig. 4. Magnified image of the specimen without diffusion barrier after diffusion couple test at 800 °C for 25 h (#1–3 magnified from the location of Fig. 3).

At the fuel side, zirconium-rich granules appeared which agglomerated with each other to form a separate layer. Such a zirconium-rich layer has a positive effect on the fuel–clad interaction. To assess the effect of the barrier layer on the diffusion behavior and the phase distribution of the diffusion-coupled specimen, a composition analysis at selective points by EDX and by collating it with a ternary phase diagram [11], was carried out, as shown in Fig. 9. For simplicity, the iron and the chromium were regarded as a single element. In the reference specimen, intermetallic compounds such as $U(Fe,Cr)_2$ and $Zr(Fe,Cr)_2$ were formed during the fuel–clad reaction. When connecting each point according to the sequence of a region, an experimental diffusion path could be obtained. Highly enriched zirconium phase, such as point b in Fig. 4(b), was not included in the diffusion path. Metallic fuel at first reacts with the iron and chromium then it converts into the liquid phase. It then changes to a zirconium-rich phase $Zr(Fe,Cr)_2$, then it gradually changes to a $U(Fe,Cr)_2$ phase along an eutectic

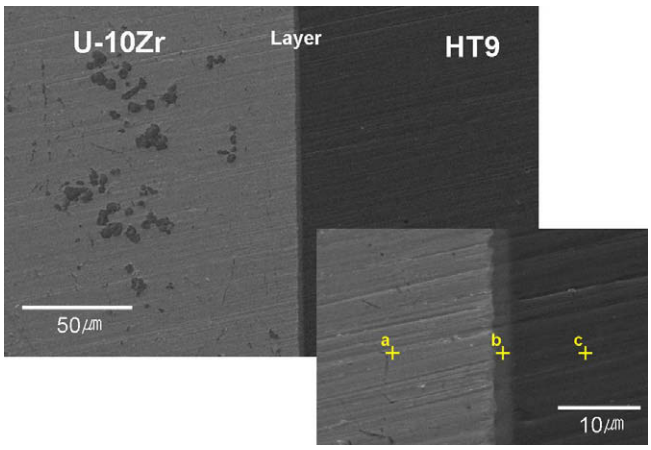

Fig. 5. Microstructure of the vapor-deposited specimen (VD #1) after diffusion couple test at 800 °C for 25 h.

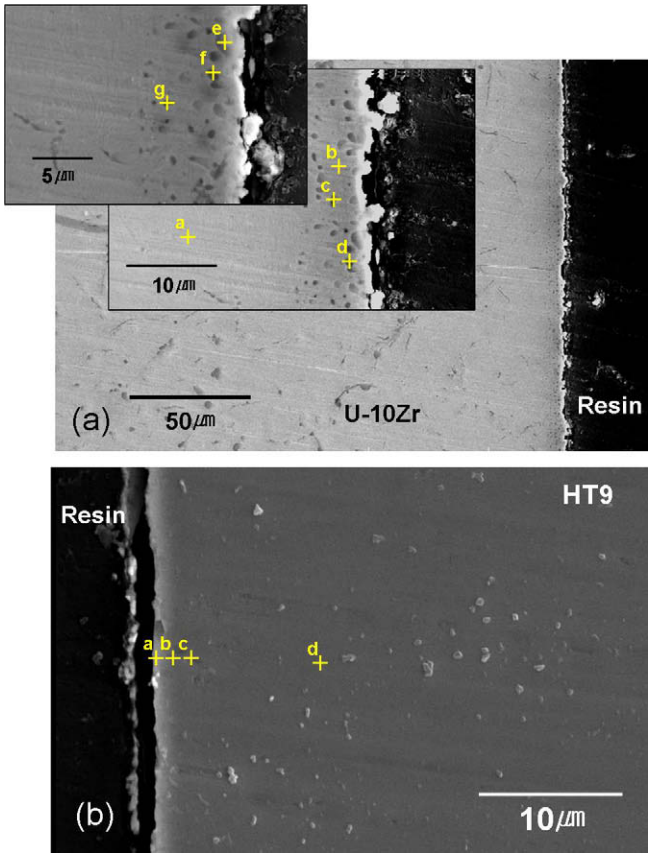

Fig. 6. Microstructure of the vapor-deposited specimen (VD #2) after diffusion couple test at 800 °C for 25 h. (a) U–10Zr side, (b) HT9 side.

line. In the vapor-deposited specimen, it was shown that a eutectic compound was not formed but γ and ε-phases were developed, showing that a reaction caused by an inter-diffusion did not occur in the case of the surface-treated specimen. Instead, a zirconium-rich phase like $Zr(Fe,Cr)_2 + Zr_2(Fe,Cr)$ phase was developed, which acted as a barrier against a FCCI.

4. Conclusion

Studies were carried out to assess the performance of the barrier layer under a FCCI. Single or multilayers of zirconium, chromium and titanium were coated onto the HT9 clad surface by the vapor deposition and diffusion couple tests at 800 °C for 25 h were performed for the U–10wt%Zr metallic fuel. Surface-treated specimens by vapor deposition were found to be resistant FCCI regardless of the coating materials. On the other hand, in a specimen without any surface treatment, a massive reaction occurred at the fuel–clad interface. The zirconium-coated layer remained intact, however multi-component-layers such as titanium, chro-

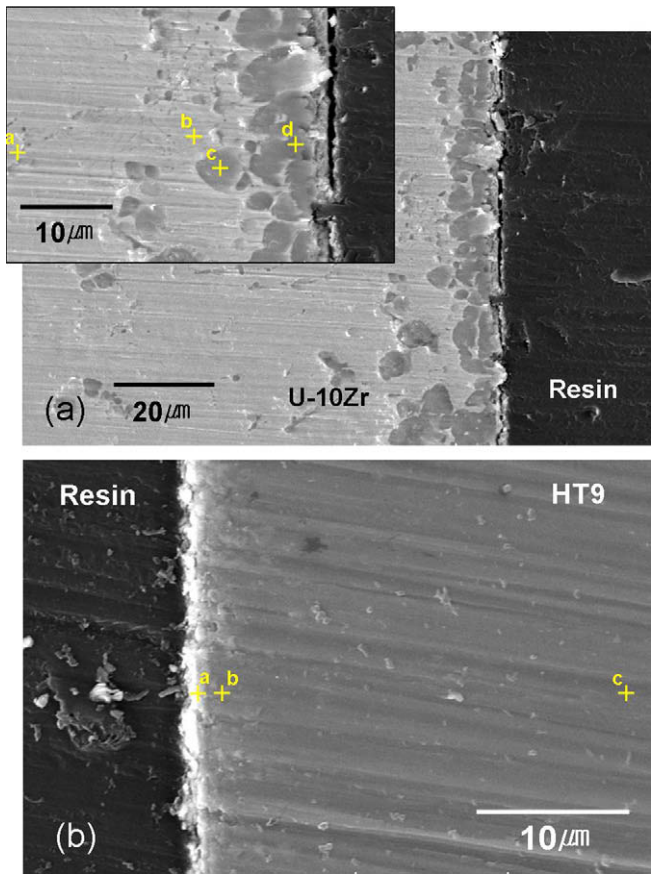

Fig. 7. Microstructure of the vapor-deposited specimen (VD #3) after diffusion couple test at 800 °C for 25 h. (a) U–10Zr side, (b) HT9 side.

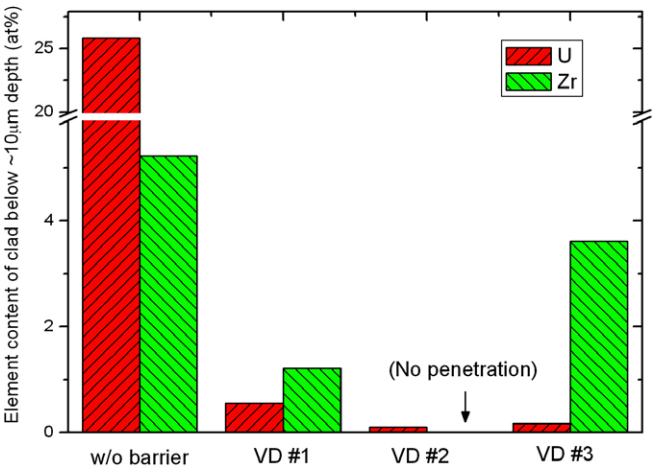

Fig. 8. Element content of the clad material below 10 μm from the interface with the vapor-deposited conditions.

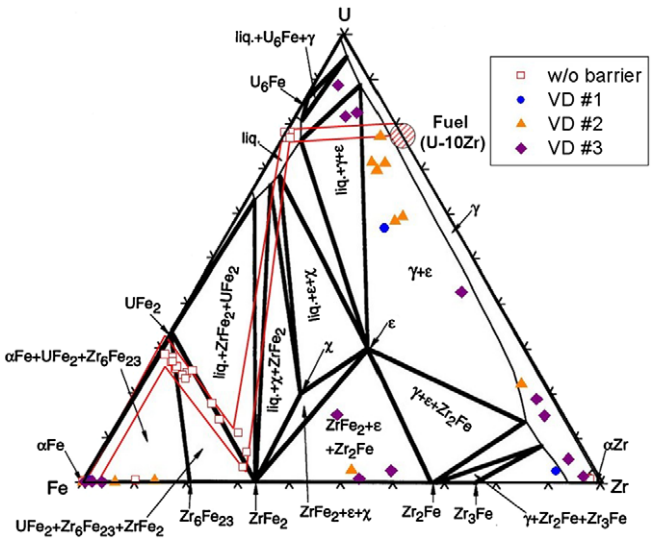

Fig. 9. Effect of the vapor deposition on the phase distribution of the metallic fuel and the clad coupled specimen after diffusion test at 800 °C for 25 h. Red line represents experimental diffusion path for the U–10 wt%Zr and HT9 clad material after diffusion test at 800 °C for 25 h. Collated phase diagram was cited after Nakamura [11]. (For interpretation of the references to color in this figure legend, the reader is referred to the web version of this article.)

mium and zirconium dissolved and formed a precipitate layer during the diffusion tests. On the other hand, secondary zirconium-rich phase preferentially agglomerated at around the precipitate layer to act as a barrier against FCCI.

Acknowledgements

This study was supported by National Research Foundation (NRF) and Ministry of Education, Science and Technology (MEST), Korean Government, through its national nuclear technology program.

References

[1] G.L. Hofman, L.C. Walkers, Metallic fast reactor fuels, in: R.W. Cahn, P. Haasen, E.J. Kramer (Eds.), Materials Science and Technology – A Compressive Treatment, 10A Part I, VCH, Germany, 1994, p. 3.
[2] D.D. Keiser Jr., M.C. Petri, Interdiffusion Between U–Pu–Zr Fuel and HT9 Cladding, CONF 940631-1, 1994.
[3] H.J. Ryu, B.O. Lee, S.J. Oh, J.H. Kim, C.B. Lee, J. Nucl. Mater. 392 (2009) 206.
[4] D. Tokiwai, R. Yuda, A. Ohuchi, M. Amaya, J. Nucl. Sci. Technol. 1 (Suppl. 3) (2002) 913.
[5] H. Fujiyama, Surf. Coat. Technol. 131 (2000) 278.
[6] W.-C. Gu, G.-H. Lv, H. Chen, G.-L. Chen, W.-R. Feng, S.-Z. Yang, Surf. Coat. Technol. 201 (2007) 6619.
[7] W.K. Halnan, D. Lee, Coatings for High Temperature Applications, Applied Science Publishers, London, 1983.
[8] S.R. Levine, R.M. Caves, J. Electrochem. Soc. 121 (1974) 1051.
[9] W. Schintlmeister, O. Pacher, J. Vac. Sci. Technol. 12 (1975) 743.
[10] M.J. Hakim, Proceedings of the Fifth Int. Conf. on Chemical Vapour Deposition, 1975, p. 634.
[11] K. Nakamura, M. Kurata, T. Ogata, A. Itoh, M. Akabori, J. Nucl. Mater. 275 (1999) 151.
[12] D.D. Keiser Jr., M.A. Dayananda, Metall. Mater. Trans. 25A (1994) 1649.
[13] D.D. Keiser Jr., M.A. Dayananda, J. Nucl. Mater. 200 (1993) 2.